Using Cortical Vessels for Patient Registration During Image-guided Neurosurgery - A Phantom Study

Hai Sun [*], David W.Roberts[†‡], Alex Hartov [*†], Kyle Rick [*], Keith D. Paulsen [*†‡]

[*]Thayer School of Engineering, Dartmouth College, NH 03755
[†]Dartmouth Hitchcock Medical Center, Lebanon, NH, 03766
[‡] Norris Cotton Cancer Center, Lebanon, NH 03766

ABSTRACT

Patient registration, a key step in establishing image guidance, has to be performed in real-time after the patient is anesthetized in the operating room (OR) prior to surgery. We propose to use cortical vessels as landmarks for registering the preoperative images to the operating space. To accomplish this, we have attached a video camera to the optics of the operating microscope and acquired a pair of images by moving the scope. The stereo imaging system is calibrated to obtain both intrinsic and extrinsic camera parameters. During neurosurgery, right after opening of dura, a pair of stereo images is acquired. The 3-D locations of blood vessels are estimated via stereo vision techniques. The same series of vessels are localized in the preoperative image volume. From these 3-D coordinates, the transformation matrix between preoperative images and the operating space is estimated. Using a phantom, we have demonstrated that patient registration from cortical vessels is not only feasible but also more accurate than using conventional scalp-attached fiducials. The Fiducial Registration Error (FRE) has been reduced from 1 mm using implanted fiducials to 0.3 mm using cortical vessels. By replacing implanted fiducials with cortical features, we can automate the registration procedure and reduce invasiveness to the patient.

Keywords: Stereopsis, patient registration, image-guided neurosurgery

1. INTRODUCTION

Pre-operative high-resolution magnetic resonance (MR) and computed tomography (CT) provide a detailed 3-D description of patient anatomy. It is desirable to align the preoperative images with the physical space in order to present the surgeon with the preoperative data correctly oriented with respect to the patient. This step is key in establishing any image-guided surgery. In mathematical terms, patient registration constructs a rigid body transformation between the pre-operative image coordinates and the coordinates in the physical OR space.

To calculate the transformation matrix that relates the preoperative image space to the patient in the OR, homologous features need to be identified in the preoperative image, and physically on the patient. At present, the quantitatively validated methods reported for patient registration involve attaching fiducials to the patient's scalp.[1–3] These points are localized in the pre-operative data space and the OR prior to surgery. From these corresponding points, the transformation matrix that aligns the preoperative images with the OR space is estimated. This method requires an extra MRI scan prior to the surgery after the fiducials are placed on the patient's scalp. The localization of these points is performed manually after the patient is anesthetized in the operating room. There is a need to automate the process for efficiency, to reduce the invasiveness of the procedure, and at the same time to achieve better accuracy.

Nakajima et. al. have demonstrated the possibility of using cortical vessels as registration landmarks.[4] In their study, the current surgical scene was captured by a video acquisition system and was displayed on a TV screen. Then, the cortical vasculature segmented from MRI was manually aligned with the current surgical

Further author information: (Correspondence should be addressed to H.S.)
H.S.: E-mail: hai.sun@dartmouth.edu, Telephone: 1 603 646 1094, fax: 1 603 646 3856
D.W.R.: E-mail: David.W.Roberts@hitchcock.org, Telephone: 1 603 650 8736
A.H.: E-mail: alex.hartov@dartmouth.edu, Telephone: 1 603 646 3936
K.R.: Email: Kyle.Rick@dartmouth.edu, Telephone: 1 603 646 1094
K.D.P.: E-mail: Keith.D.Paulsen@dartmouth.edu, Telephone: 1 603 646 2695

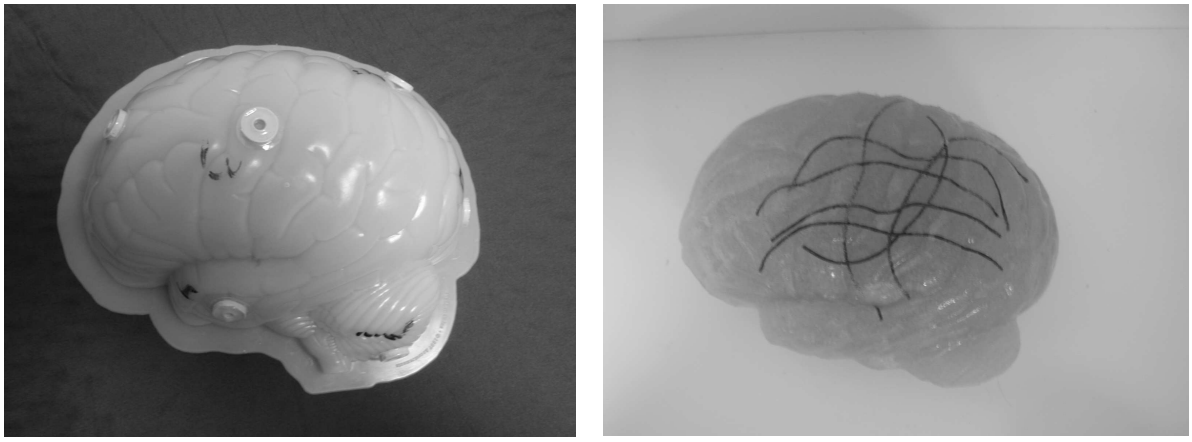

Figure 1. Brain phantom employed to quantitatively validate patient registration using cortical vessels. The image on the left shows the brain mold with attached patient registration fiducials, and the image on the right shows that the brain phantom with cortical vessels simulated by electric wires.

scene to evaluate the surgical trajectory. The operating microscope optics were not calibrated, hence this implementation required significant human intervention and the evaluation of system performance remained qualitative.

We propose to use cortical vessels as landmarks for registering the preoperative images to the operating space. By replacing implanted fiducials with cortical features, we hope to automate the registration procedure and reduce the invasiveness to the patient. In order to register the patient with cortical vessels, the same group of vessels has to be localized both in image and OR spaces. The operating microscope is used to recover the 3-D location of cortical vessels in the OR space. A suitable technique for obtaining the range estimation of the cortical surface is stereopsis.

Then, the same group of vessels are segmented from the preoperative images using a semi-automatic strategy. From these 3-D coordinates, the transformation matrix between preoperative images and the operating space is estimated. Using a phantom, we have demonstrated that patient registration from cortical vessels is not only feasible but also more accurate. The Fiducial Registration Error (FRE) has been reduced from 1 mm using implanted fiducials to 0.3 mm using cortical vessels.

2. METHODS

This section is divided into three parts: image generation and segmentation, range estimation, and registration of 3-D data.

2.1. Image Generation and Segmentation

The goal of this step is to obtain the 3-D coordinates of cortical vessels in the preoperative image space. For the purpose of quantitatively validating our method, we have implemented a brain shaped phantom. We use a jello mold in the shape shown in figure 1(obtained from the Red Roof Publications online website [5]). We placed several electric wires to simulate cortical vessels at the bottom of the mold, then poured agar gel into the mold. Once solidified, it resembles a human brain. We also attached the fiducial markers we use in patient cases onto the outside surface of the brain mold. Finally, a CT scan of the mold containing the solidified gel brain was obtained.

The "cortical vessels", simulated by the electric wires were segmented in the CT data using thresholding. The 3-D coordinates of these voxels in the pre-operative images space were obtained.

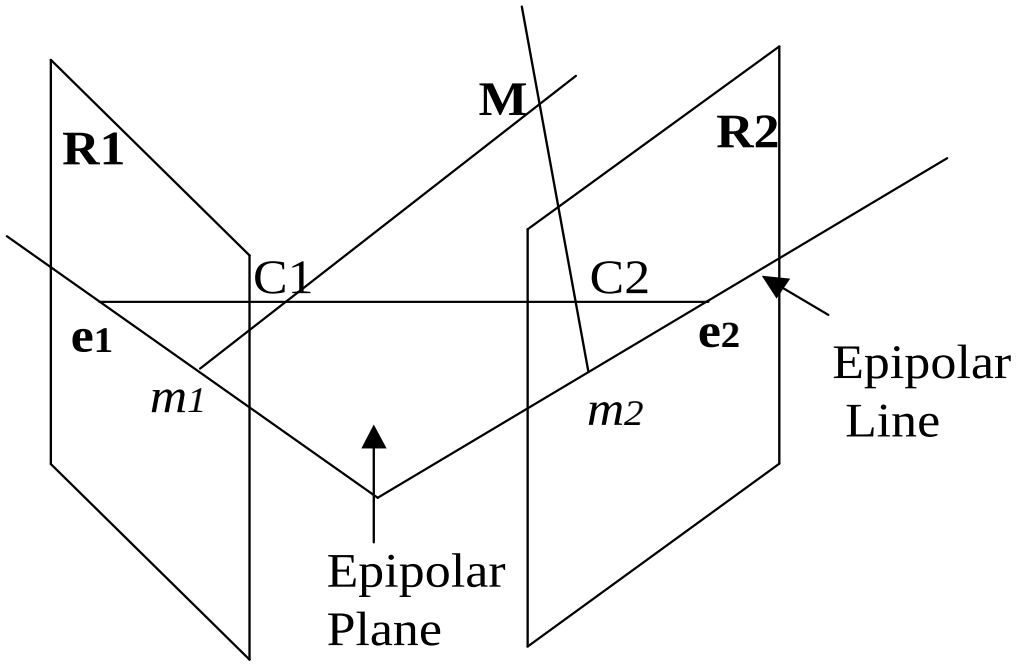

Figure 2. The 3-D vision problem and the epipolar constraint: two pinhole cameras form the image m_1 and m_2 of a physical point M. C_1 and C_2 are two camera centers. According to the epipolar constraint, the correspondence point of m_1, m_2, is constrained to lie on the epipolar line of m_1 on R2, which is defined as the projection of the optical ray of m_1 through the right camera center, C_2. The epipolar plane is defined by the epipolar line of m_1 and the epipolar line of m_2.

2.2. Range Estimation

The goal of this step is to obtain the 3-D coordinates of cortical vessels in the OR space. The relative displacement or disparity in the position of objects, as viewed by a pair of eyes, is an important source of depth information for humans. This phenomenon, termed binocular stereopsis, can be used to recover some of the 3-D information present in the scene. A survey of methods has been provided by Dhond et al.[6] An implementation of this technique for improving image-guided neurosurgery was proposed by Skrinjar et. al., who tried to solve the correspondence problem through the Lambertian characteristics.[7]

The basic concept of stereo vision is illustrated in figure 2: two pinhole cameras form the image m_1 and m_2 of a physical point M. C_1 and C_2 are two camera centers. The problem of stereo vision can be divided into two stages:

1. For a point m_1 in plane R1, decide its correspondence point m_2 in plane R2. Here, correspond means that they are the images of the same physical point M. This is termed the correspondence problem.

2. Given m_1 and m_2, compute the 3-D coordinates of M in the world reference frame. This is called the reconstruction problem.

Shown in figure 3 is the stereo imaging system we employed to digitize the cortical surface. At the current stage, one Sony video camera is mounted on the operating microscope (Model M695, Leica USA, Rockleigh, NJ). Two images of a stereo pair can be recorded by moving the microscope. The first image is digitized with the microscope at one location, and another image s acquired with the scope at a slightly different location. The positions of the microscope were recorded with a optical tracking system.

With the simple model, shown in figure 2, the second stage of stereopsis can be completed by finding the intersection of the lines $\langle C_1, m_1 \rangle$ and $\langle C_2, m_2 \rangle$. This result relies on how accurately we calibrated the camera

Figure 3. Stereopsis is achieved by the motion of the operating microscope. The arrow on the left indicates that a video camera has been attached to one microscope ocular. The arrow on the right indicates that an Infra Red Emitting Diode (IRED) tracker has been rigidly attached to the microscope to track its position and orientation. A stereo image pair was formed by acquiring two images with the microscope at two different locations. These locations were recorded by the tracker.

system. Standard camera calibration[8] yields both intrinsic and extrinsic camera parameters of the microscope. The intrinsic parameters are the focal length, camera center, and image aspect ratio. In our case, these parameters define the mapping from 3-D microscope frame to 2-D microscope image coordinates. The extrinsic parameters relate the 3-D microscope frame to the 3-D coordinate system of a fixed (and arbitrary) calibration system via a rigid-body transformation.

The first stage is more difficult. Its difficulty arises from the fact that the correspondence problem is ambiguous: Given a point m_1 in R1, it may a priori be put in correspondence with any point m_2 in R2. To solve this difficulty, we have implemented three matching constraints to reduce the number of potential matches for any given point m_1.[6, 9, 10]

To begin, we first need to locate the cortical vessels in one image of the stereo pair and use these pixels as matching tokens. In order to segment the cortical vessel from video images, we applied a gray-level threshold. Since cortical veins are generally darker than the surrounding brain tissues, this method has produced correct matching tokens in some cases. When the threshold strategy failed, we manually traced the shape of the simulated cortical vessels. Each vessels are fitted with a B-spline. All pixels that were traversed by a B-spline were selected as tokens. Then, the following matching constraints were applied to establish correspondence.

1. The Epipolar Constraint

   This is probably the most important geometric constraint imposed by the imaging system. If we add some drawings to figure 2, the epipolar constraint can be easily demonstrated. Let's first construct the epipolar line of m_1, which is defined as the projection of the optical ray of m_1 through the right camera center, C_2. Now, the correspondence point of m_1, m_2, is constrained to lie on the epipolar line of m_1 on R2. The epipolar plane is defined by the epipolar line of m_1 and the epipolar line of m_2.

The stereo matching problem can be solved much more efficiently if images are rectified. This step consists of transforming the images so that the epipolar lines are aligned with pixel rows. In this case stereo matching algorithms can easily take advantage of the epipolar constraint and reduce the search space to one dimension (i.e. corresponding rows of the rectified images).[9–11] After the calibration of the stereo system, both intrinsic and extrinsic camera parameters are used to define two new perspective matrices which preserve the optical centers but with image planes parallel to the baseline. In addition the epipolar line of a point in the right image is made to be a horizontal line in the left image.

2. An Intensity Correlation Constraint

   We have adopted a measure based on the grey-levels in the image: The input is a rectified stereo pair I_l (left) and I_r. Let P_l and P_r be pixels in the left and right image, 2W+1 the width(in pixels) of the correlation window, $R(P_l)$ the search region in the right image associated with P_l, and $\psi(u, v)$ a function of two pixel values u, v. For each pixel $P_l = [i, j]^\top$ of the left image:

   - for each displacement $d = [d_1, d_2]^\top \in R(P_l)$ compute

$$c(d) \;=\; \sum_{k=-W}^{W} \sum_{l=-W}^{W} \psi(I_l(i+k, j+l), I_r(i+k-d_1, j+l-d_2)); \tag{1}$$

   - the disparity of P_l is the vector $\bar{d} = [\bar{d_1}, \bar{d_2}]^\top$ that maximizes $c(d)$ over $R(P_l)$:

$$\bar{d} \;=\; arg \max_{d \in R} c(d) \tag{2}$$

     When the images are rectified, d_1 is equal to zero and the search is constrained to one dimension. The output is an array of disparities (the disparity map), one per each pixel of I_l. Our choice for the function $\psi = \psi(u, v)$ in equation 1 is

$$\psi(u, v) \;=\; -(u - v)^2, \tag{3}$$

     which performs the so called SSD (sum of squared differences) or block matching.[10]

3. The Left-Right Consistency Constraint

   Since the cortical surface is relatively smooth and opaque, the microscope is close to the brain, and the left and right optical rays form a small angle (less than 15°), a continuity constraint, the left-right consistency constraint, can be applied to further assure accurate matching. Only corresponding pairs found matching left-to-right and right-to-left are accepted. Spurious matches, i.e., false corresponding pairs created by noise, can be eliminated by applying this constraint.

After the correspondence problem is solved, each pair of homologous points is combined with the optical centers to form two rays. In theory, the intersection of these two rays is the desired 3-D coordinate. In reality, since camera parameters and image locations are known only approximately, the two rays will not actually intersection in space. Their intersection can only be estimated as the point of minimum distance from both rays.[10] After completing this step, we now have obtained the 3-D coordinates of cortical vessels in the OR space.

2.3. The Registration of the 3-D Coordinates

Equipped with the 3-D coordinates of the same set of cortical vessels in both preoperative image space and the OR space, we now can estimate the transformation matrix to register the patient. An iterative closest point (ICP) technique [12,13] is employed to compute this matrix. The ICP algorithm, given an initial translation and rotation, converges monotonically to the nearest local minimum of a mean-square distance metric. The problem with reaching the desired global minimum with certainty can be solved by applying an adequate set of initial rotations and translations. In our phantom studies, the ICP algorithm has successfully estimated the transformation matrix between image and patient spaces with less than 6 randomized initial guesses.

Because the ICP algorithm is a shape-based registration strategy, the rigid-body transformation can be estimated without one-to-one match between the two groups of 3-D coordinates. When using cortical vessels to register a patient, we can usually obtain a larger number of coordinates in the preoperative image space. After image segmentation, all of the voxels that belongs to cortical vessels in the vicinity of the craniotomy site are chosen. The ICP algorithm is capable of finding a subset of points among all of the chosen voxels and matching these points with 3-D coordinates reconstructed via stereopsis. The transformation matrix is then estimated with these matched coordinates. Furthermore, a threshold-based strategy can be implemented and incorporated into ICP to select points that warrant a better shape-based registration.

3. RESULTS

In this section, we will first present the validation of range estimation via stereopsis. Then the metrics for measuring patient registration error will be listed for the two registration strategies, i.e., using cortical vessels as fiducials and using conventional scalp-attached fiducials. Finally, the results using these two strategies from a clinical case will be compared.

3.1. Validation of Stereopsis

In order to quantify the performance of the implemented matching constraints, an experiment followed by a numerical simulation was designed and executed to probe the error in range estimation as a result of error in solving the correspondence problem. An accurately manufactured calibration target consisting of numerous fiducial marker with known relative positions was brought into the OR. The target was tracked, so that the locations of its features were known. At the beginning of the experiment, the camera was calibrated. The stereo image pair was formed by microscope motion, which was recorded via our 3-D tracking system. The camera calibration results and microscope tracking data were used to rectify the stereo image pairs. The centroids of markers in both the left and right images were estimated via segmentation and each corresponding pair were matched manually. Then the triangulation produced the 3-D coordinates of these centroids and the RMS error was estimated by comparing the results with the locations of these centroids recorded by the Polaris system. The homologous points were estimated via segmentation and matched manually, we consider that there is no matching error introduced by this process. The RMS error of range estimation was determined solely by errors from camera calibration and tracking.

Then we simulated matching error (pixels) in either the x or y image axis by altering the estimated locations of centroids in the right image. The RMS error of the range estimation based on altered homologous pairs was computed. Figure 4 shows the relationship between RMS errors in range estimation and simulated matching errors. The simulated results have shown that the matching errors in x are more significant in causing an increase of error in range estimation than the same errors in y. Our interpretation of this result is that, in order to achieve more accurate range estimation, matching constraints must be able to solve correspondence with subpixel accuracy in the x direction, and in y, however, the performance of these constraints can be allowed some tolerance. In order to achieve this requirement, two of the three matching constraints implemented, i.e., the intensity correlation constraint and the left-right consistency constraint, are designed to reinforce the matching accuracy in the x direction. After image rectification, the search for a potential match was generally widened to include 3-5 lines of pixels adjacent the epipolar lines to counter potential matching errors in the x direction that may be a result of inaccurate rectification.

3.2. Phantom Studies

Phantom experiments were conducted in the operating room. Before the mold was taken off the brain phantom, the attached fiducials were digitized with the 3-D tracking system. After the removal of the mold, the cortical vessels simulated by electric wires were exposed. Stereo image pairs were formed by microscope motion and recorded. Camera locations were recorded. To recover the location of these vessels, first, a threshold was applied to the left image to extract matching tokens. To increase the efficiency of the algorithm, only one-third of the matching tokens were selected. Then, three matching constraints were applied to find the homologous points in the right image. Shown in figure5 is the result of matching. Then the established correspondence, when combined with the camera calibration, yields the desired 3-D coordinates. The cortical vessels in the preoperative CT were

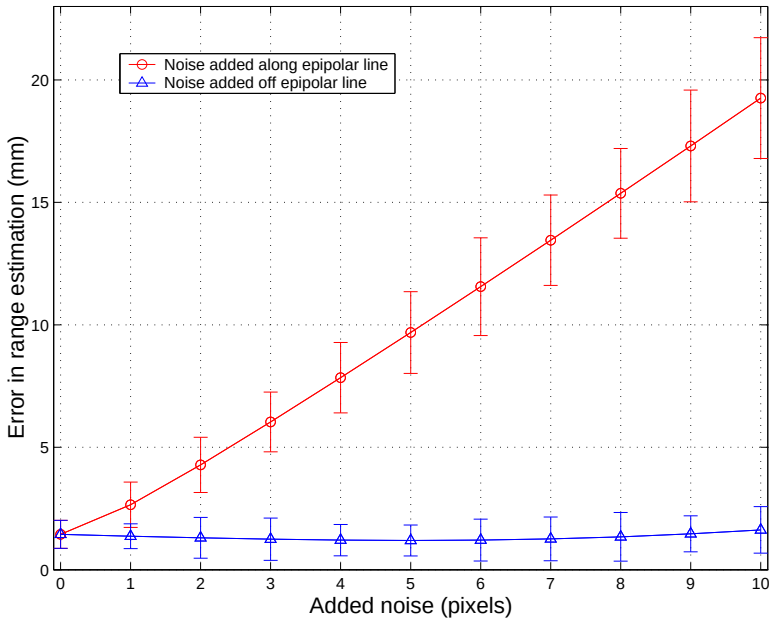

Figure 4. The simulated results of range estimation. The 3-D coordinates of centroids of markers on a accurately manufactured target were estimated initially based on matching obtained by segmenting the same image feature in both left and right image. Errors in either x or y image axis were subsequently added to the matching results. RMS errors of range estimation based on matching with and without added errors were computed and plotted. Figure (a) is a plot of RMS errors in range estimation vs. matching errors in x axis and figure (b) RMS errors vs. matching errors in y.

Registration Type	Number of fiducials	FRE (mm)	TRE (mm)
Using conventional fiducials	7	0.99	0.51
Using cortical vessels	57	0.26	0.05

Table 1. Results of phantom studies: FREs and TREs of patient registration using the conventional scalp-attached fiducials and using cortical vessels

segmented by thresholding, the ICP algorithm was applied to estimate the transformation matrix between the preoperative image space and the patient, i.e., phantom space in the OR. The same matrix was also estimated via the conventional patient registration technique. The two metrics, fiducial registration error (FRE) and target registration error (TRE) were employed to compare these two techniques.[14] The results are shown in table 1.

4. DISCUSSION

Through numerical simulations and phantom studies, we have demonstrated in these early efforts that using cortical vessels to perform patient registration is a possible alternative strategy to the conventional method using scalp-attached fiducials with obvious advantages, such as no requirement for an extra MRI scan with fiducials, less invasiveness to the patient, and the possibility for automation.

In order for our system to be viable in a clinical setting, several challenges have to be overcome. First, we would like to improve the accuracy of range estimation by implementing binocular stereopsis. Shown in figure 4, without any matching error, the best performance of our current range estimation via stereopsis produces an average RMS error on the order of 1.5 mm. With homologous points accurately localized in a stereo pair, the error in range estimation is mainly introduced in the step of triangulation, where camera parameters and locations are used to recovered the 3-D location of objects in the image. In our current system, a stereo image pair is generated by the motion of microscope attached with one camera. Since the two locations of the microscope where each of the images is formed are used for triangulation, the contribution of inaccuracy in tracking the microscope to the error in range estimation are considerable. A strategy to reduce the error requires a binocular stereopsis.

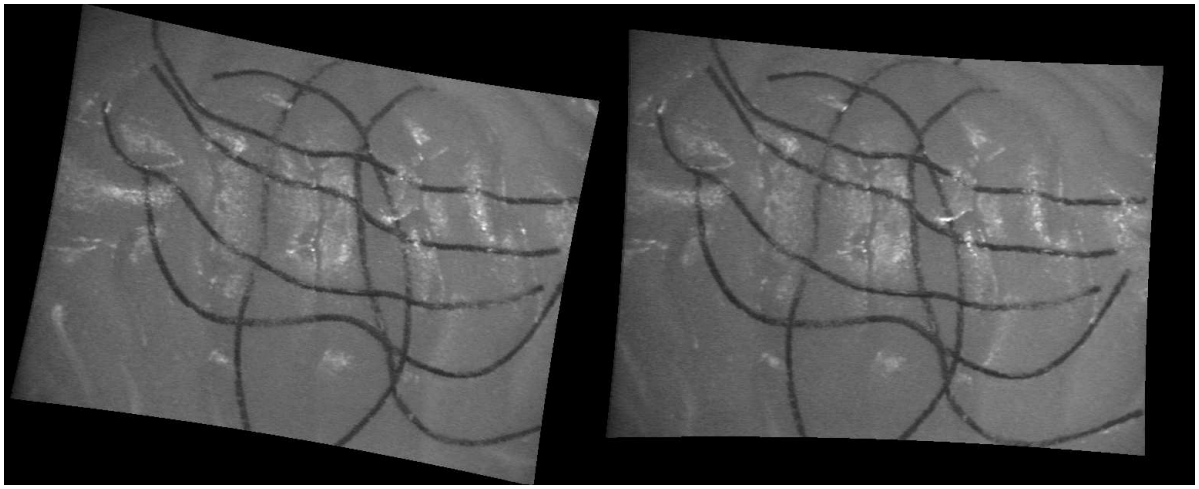

(a)

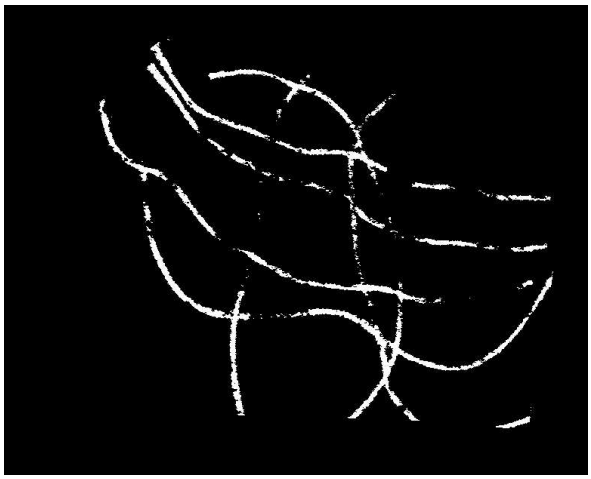

(b)

Figure 5. Rectification and Feature Matching with images of brain phantom. Image (a) shows the rectification results of a pair of stereo images. Image (b) shows the resulting disparity map: only pixels associated with vessels are chosen for matching. Large disparities correspond to small values of the intensity, small disparities to large intensity values. Since the cortical surface is relatively smooth, the disparities vary little.

The operating microscope is equipped with binocular vision. We plan to attach a CCD camera to each ocular, so that a stereo image pair can be formed without moving the microscope. The binocular stereo will also enable image rectification without knowledge of the physical location of the microscope. The new perspective matrices to rectify an image pair can be obtained through the initial calibration and maintained during a clinical case.[9–11] Another avenue for improving the performance of a stereo system is to utilize cameras with higher resolution.

Second, image segmentation and feature identification needs automation. In order to recover the 3-D location of cortical vessels in the OR, pixels that belongs to these vessels have to be selected as matching tokens. In addition, these same set of vessels need to be identified and localized in the preoperative images. Successful image segmentation and feature identification are key for using cortical vessels to register patient. A wealth of literature can be found on this subject.[15–17] Most strategies are only successful given images with specified quality and intensity or color distribution, whereas medical images vary a great deal in these characteristics. We have been able to automate this process in our phantom studies, but the automation in clinical cases remains a challenge.

Third, in our phantom studies, we were able to show that more accurate co-registration has been achieved by using cortical vessels for patient registration than by using scalp-attached fiducials, which is reflected by the two conventional metrics, Fiducial Registration Error(FRE) and Target Registration Error (TRE). These results concur with the observation that cortical vessels are in greater proximity and spatial constancy with respect to the target of interest (tumor, etc.). However, in some cases, where the size of craniotomy is small enough to limit the amount of exposed cortical vessels, the registration points obtained from these vessels may not have an optimal spatial distribution. This can lead to an increase in registration errors or even the failure of this strategy. In these instances, features within the brain need to be added to the group of registration fiducials to achieve better results.

ACKNOWLEDGMENTS

The project is funded by the National Institute of Neurological Disorders and Stroke (NINDS, R01-NS33900).

REFERENCES

1. P. Edwards, A. King, C. M. Jr., D. Hawkes, D. Hill, R. Gaston, M. Fenlon, A. Jusczyzck, A. Strong, C. Chandler, and M. Gleeson, "Design and evaluation of a system for microscope-assisted guided interventions (MAGI)," *IEEE Trans. on Med. Imaging* **19**, pp. 1082–1093, 2000.
2. C. Maurer, M. Fitzpatrick, M. Wang, J. R.L. Galloway, R. Maciunas, and G. Allen, "Registration of head volume images using implantable fiducial markers," *IEEE Trans. on Med. Imaging* **16**, pp. 447–462, 1997.
3. J. West, J. Fitzpatrick, M. Wang, J. B.M. Dawant, C.R. Maurer, R. Kessler, and R. Maciunas, "Retrospective intermodality registration techniques for images of the head: Surface-based versus volume-based," *IEEE Trans. on Med. Imaging* **18**, pp. 144–150, 1999.
4. S. Nakajima, H. Atsumi, R. Kikinis, T. Moriarty, D. Metcalf, F. Jolesz, and P. Black, "Use of cortical surface vessel registration for image-guided neurosurgery," *Neurosurgery* **40**, pp. 1201–1210, 1997.
5. R. R. Publications, "Brain mold." webpage. http://www.redreef.com/mold.html.
6. U. Dhond and J. Aggarwal, "Structure from stereo - a review," *IEEE Trans. on Systems, Man and Cybernetics* **19**, pp. 1489–1510, 1989.
7. O. Skrinjar, H. Tagare, and J. Duncan, "Surface growing from stereo images," *IEEE Computer Society Conference on Computer Vision and Pattern Recognition (CVPR 2000)* , pp. 571–576, 2000.
8. R. Y. Tsai, "A versatile camera calibration technique for high-accuracy 3-D machine vision metrology using off-the-shelf TV cameras and lenses," *IEEE J. Robot. Automat.* **3**, pp. 323–344, 1987.
9. O. Faugeras, *Three-dimensional Computer Vision*, MIT Press, Cambridge, MA, 1993.
10. E. Trucco and A. Verri, *Introductory Techniques for 3-D Computer Vision*, Prentice Hall, Upper Saddle River, NJ, 1998.
11. D. V. Papadimitriou and T. J. Dennis, "Epipolar line estimation and rectification for stereo images pairs," *IEEE Transactions on Image Processing* **3**, pp. 672–676, 1996.
12. P. Besl and N. McKay, "A method for registration of 3-D shapes," *IEEE Trans. on Pattern Analysis and Machine Intelligence* **14**, pp. 239–256, 1992.
13. S. Lavallee and R. Szeliski, "Recovering the position and orientation of free-form objects from image contrours using 3D distance maps," *IEEE Trans. on Pattern Analysis and Machine Intelligence* **17**, pp. 378–390, 1995.
14. J. M. Fitzpatrick, J. B. West, and J. C. R. Maurer, "Predicting error in rigid-body point-based registration," *IEEE Trans. on Med. Imageing* **17**, pp. 694–702, 1998.
15. R. Malladi, J. Sethian, and B. Vemuri, "Shape modeling with front propagation: A level set approach," *IEEE Trans. on Pattern Analysis and Machine Intelligence* **17**, pp. 158–175, 1995.
16. M. Kass, A. Witkin, and D. Terzopoulos, "Snakes: Active contour models," *International Journal of Computer Vision* , pp. 321–331, 1988.
17. Y. Sato, S. Nakajima, N. Shiraga, H. Atsumi, S. Yoshida, T. Koller, G. Gerig, and R. Kikinis, "Three-dimensional multi-scale line filter for segmentation and visulization of curvilinear structures in medical images," *Medical Image Analysis* **2**, pp. 143–168, 1998.